Temperature field of the Mallik gas hydrate occurrence — implications on phase changes and thermal properties

J. Henninges[1], J. Schrötter[1], K. Erbas[1], and E. Huenges[1]

Henninges, J., Schrötter, J., Erbas, K., and Huenges, E., 2005: Temperature field of the Mallik gas hydrate occurrence — implications on phase changes and thermal properties; in *Scientific Results from the Mallik 2002 Gas Hydrate Production Research Well Program, Mackenzie Delta, Northwest Territories, Canada, (ed.) S.R. Dallimore and T.S. Collett; Geological Survey of Canada, Bulletin 585, 14 p.*

Abstract: Three 1200 m deep wells, spaced at 40 m, were equipped with permanent fibre-optic sensor cables. The variation of temperature within a continental, permafrost-associated gas hydrate occurrence was measured deploying the distributed temperature-sensing technology. Analysis of the transient temperature changes induced by the drilling and completion of the wells indicates that the base of the ice-bearing permafrost and the base of the gas hydrate occurrences is 604–609 ± 3.5 m, and 1108–1109 ± 3.5 m, respectively. Twenty-one months after the completion of the boreholes, the well temperatures are within ± 0.1 °C of equilibrium with the formation temperature. The analysis of the geothermal gradient shows that high gas hydrate saturations within the pore space have only a minor effect on the bulk-rock thermal conductivity compared to changes in lithology.

Résumé : Trois puits de 1 200 m de profondeur, espacés de 40 m, ont été instrumentés avec des câbles-sondes permanents à fibres optiques permettant par détection thermique simultanée (*distributed temperature sensing*) de mesurer les variations de température dans une accumulation continentale d'hydrates de gaz associée à du pergélisol. L'analyse des changements transitoires de température occasionnés par le forage et l'achèvement des puits indique que la base du pergélisol contenant de la glace se situe entre 604 et 609 ± 3,5 m, alors que la base de la zone d'hydrates de gaz se trouve entre 1 108 et 1 109 ± 3,5 m. Vingt et un mois après l'achèvement des forages, les températures mesurées dans les puits s'écartaient d'un maximum de ± 0,1 °C de l'équilibre avec la température des sédiments. L'analyse du gradient géothermique montre que, comparativement aux changements lithologiques, la forte saturation en hydrates de gaz de l'espace interstitiel a un effet mineur sur la conductivité thermique globale des formations.

[1]GeoForschungsZentrum Potsdam, Telegrafenberg, 14473 Potsdam, Germany

INTRODUCTION

The size and distribution of natural methane hydrate occurrences and the release of gaseous methane through the dissociation of methane hydrate are predominantly controlled by the subsurface pressure and temperature conditions. This field experiment was carried out within the framework of the Mallik 2002 Gas Hydrate Production Research Well Program, investigating the in situ conditions of one of the most concentrated gas hydrate occurrences currently known, located at the coast of the Mackenzie Delta, Northwest Territories, Canada (Dallimore and Collett, 2005). A thick permafrost layer extending to a depth of about 600 m below ground level overlies gas hydrate accumulations between about 800 m and 1100 m below ground level within the sedimentary succession.

Previously, the analysis of the geothermal conditions and the derivation of the stability field for methane hydrate at the Mallik site were based on the interpolation of single, thermally disturbed, bottom-hole temperature measurements and drill-stem test data from petroleum exploration wells (Majorowicz and Smith, 1999). Within permafrost environments, the depth to the base of the permafrost is often used as a constraint to the subsurface temperature field (Majorowicz et al., 1990). Taylor and Judge (1981) evaluated different methods of measuring and predicting permafrost thickness. On the basis of a large collection of temperature data, Judge et al. (1987) estimated the depth to base of ice-bearing permafrost in the Mackenzie Delta–Beaufort Sea region. Dallimore and Collett (1999) and Dallimore et al. (1999) estimated the depth to the ice-bearing permafrost at the Mallik site according to geophysical well logs of the Mallik L-38 and 2L-38 wells. Within the present study, the transient temperature response of a well drilled in permafrost (Lachenbruch and Brewer, 1959; Taylor, 1979) was used for the determination of the depth to base of ice-bearing permafrost at the Mallik 3L-38, 4L-38, and 5L-38 wells. For the first time, the same method was applied to determine the base of the gas hydrate occurrences.

In cases where measurements of the formation temperature are not available, estimates of the geothermal gradient are often derived from local heat flow and the thermal conductivity of the formation. Apart from the importance for the subsurface temperature field, the thermal properties of gas-hydrate-bearing rocks are a controlling factor for all processes involving the formation and decomposition of gas hydrate in nature, which is inevitably coupled with the transport of heat within the formation. It has often been proposed that the presence of gas hydrate should have a significant influence on the bulk-rock thermal conductivity and the geothermal gradient within gas-hydrate-bearing formations (e.g. Ruppel, 2000). Until now, only a limited number of laboratory measurements on artificially produced samples have been published and there is a lack of measurement data from field samples. Stoll and Bryan (1979) performed measurements of the thermal conductivity of mixtures of sand, water, gas, and gas hydrate. Waite et al. (2002) presented thermal conductivity data for varying percentages of gas hydrate content in porous mixtures of methane hydrate and quartz sand. On the basis of the acquired temperature data, implications on the thermal conductivity of the gas-hydrate-bearing sediments at Mallik are presented.

Beside the information about the geothermal field, the online temperature monitoring has delivered important data for the thermal stimulation test, which was performed in the Mallik 5L-38 well, the results of which will be published elsewhere (e.g. Hancock et al., 2005).

FIBRE-OPTIC DISTRIBUTED TEMPERATURE MEASUREMENTS

During the field experiment, the temperature variations along the central production well (JAPEX/JNOC/GSC Mallik 5L-38) and the two lateral observation wells (JAPEX/JNOC/GSC Mallik 3L-38 and 4L-38) were measured. Through the deployment of fibre-optic distributed temperature sensing (DTS) technology, quasi-continuous temperature profiles can be measured with high temporal resolution (Wisian et al., 1998).

The principle of distributed temperature sensing was described in Hartog and Gamble (1991); examples for the application in boreholes were given in Hurtig et al. (1993) and Förster et al. (1997). The DTS system (opto-electronic unit manufactured by Sensa, United Kingdom, model DTS 800 M10) deployed in this study enabled the simultaneous online registration of temperature profiles along the three boreholes with a maximum accuracy of ± 0.3°C. Prior to and during the field experiment, individual calibrations of the deployed sensor cables were performed in a temperature-controlled chamber at the GeoForschungsZentrum Potsdam and on the Mallik site.

Installation of sensor cables

A special feature of the experiment design is the permanent installation of the sensor cables outside the borehole casing. After completion of the well, the sensor cables are located in the cement annulus between casing and borehole wall (*see* Fig. 1–3).

The fibre-optic cables were attached to the outer side of the casing at every connector, at intervals of approximately 12 m, using custom-built cable clamps. In the Mallik 3L-38 and 4L-38 wells, the sensor cables were installed to a depth of approximately 1160 m, and in the Mallik 5L-38 well temperatures could be measured to about 940 m depth (*see* Table 1 and discussion in Appendix below). All depth data in this paper relating to the Mallik 3L-38, 4L-38, and 5L-38 wells are relative to rotary kelly bushing (KB), which was 4.6 m above ground level, unless otherwise stated. In order to enable a smooth sequence of operations during the running of the casing, as well as to avoid damage to the sensor cable during the handling on the rig floor, every step of the installation was carefully planned and co-ordinated with the drilling engineers and crew. Despite the precautions, damages to the sensor cables in the Mallik 4L-38 and 5L-38 wells did occur. Nevertheless, the logging schedule was completed as planned, and high-quality temperature data were obtained from all three wells. Further details of the experimental design are discussed in the Appendix.

Government regulations for the abandonment procedure required that the wells be plugged and the casing cut below ground level. In order to enable future temperature measurements,

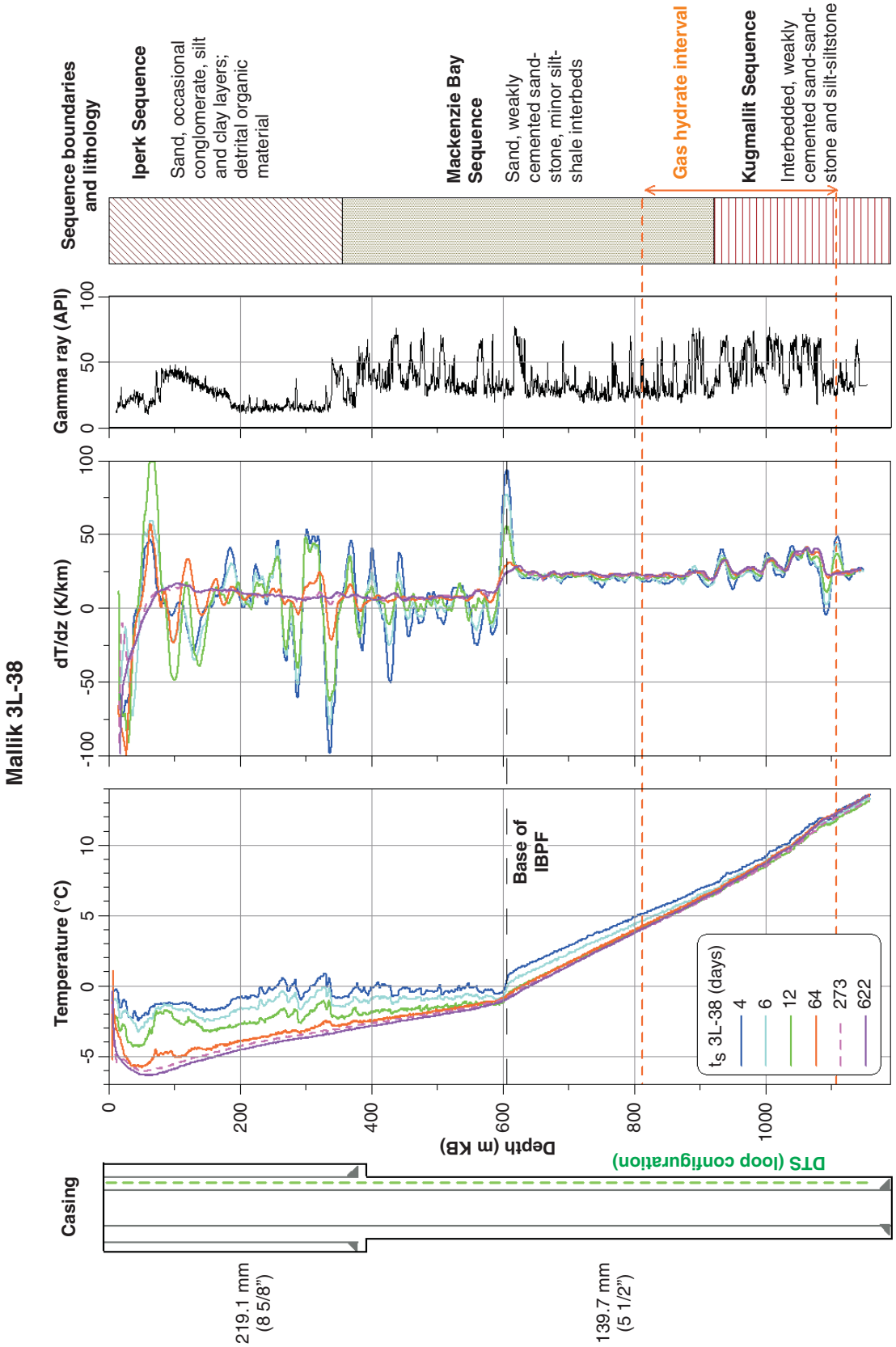

Figure 1. *Temperature profiles (T) and 20 m average temperature gradient (dT/dz) of the Mallik 3L-38 observation well for successive times after completion of the well (t_S). The base of the ice-bearing permafrost (IBPF) and gas hydrate occurrences are respectively marked by a sinusoidal change of the temperature gradient, which gradually diminishes with time. The gamma-ray response (GR) is affected by the casing (cased-hole log). Sequence boundaries and lithological description* modified from *Dallimore et al. (1999). Day 273 temperature profile: uncertain calibration. Depth in metres below kelly bushing (m KB).*

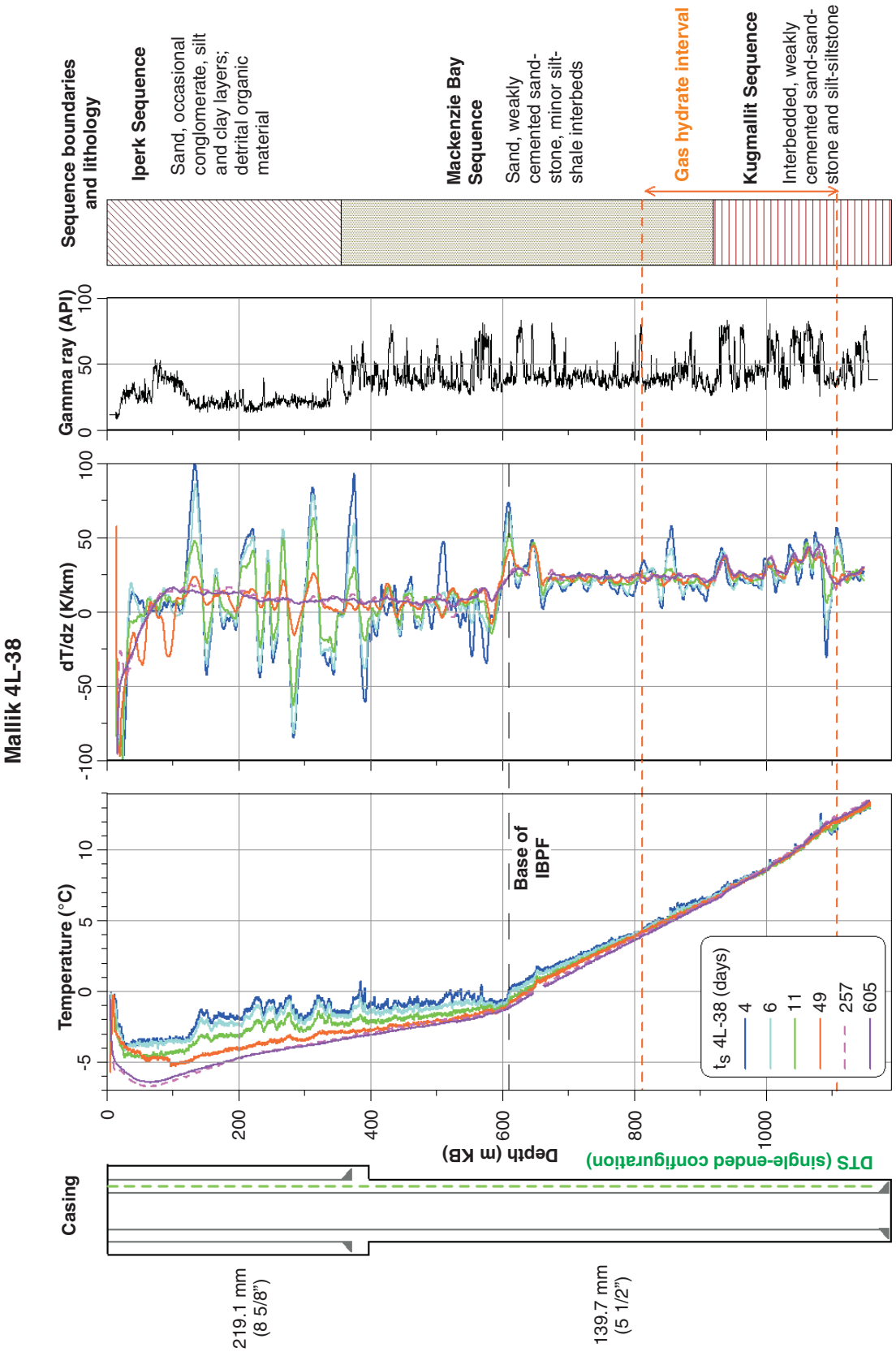

Figure 2. *Temperature profiles (T) and 20 m average temperature gradient (dT/dz) of the Mallik 4L-38 observation well for successive times after completion of the well (t_s). IBPF: ice-bearing permafrost. The gamma-ray response (GR) is affected by the casing (cased-hole log). Sequence boundaries and lithological description* modified from *Dallimore et al. (1999). Day 257 temperature profile: uncertain calibration. Depth in metres below kelly bushing (m KB).*

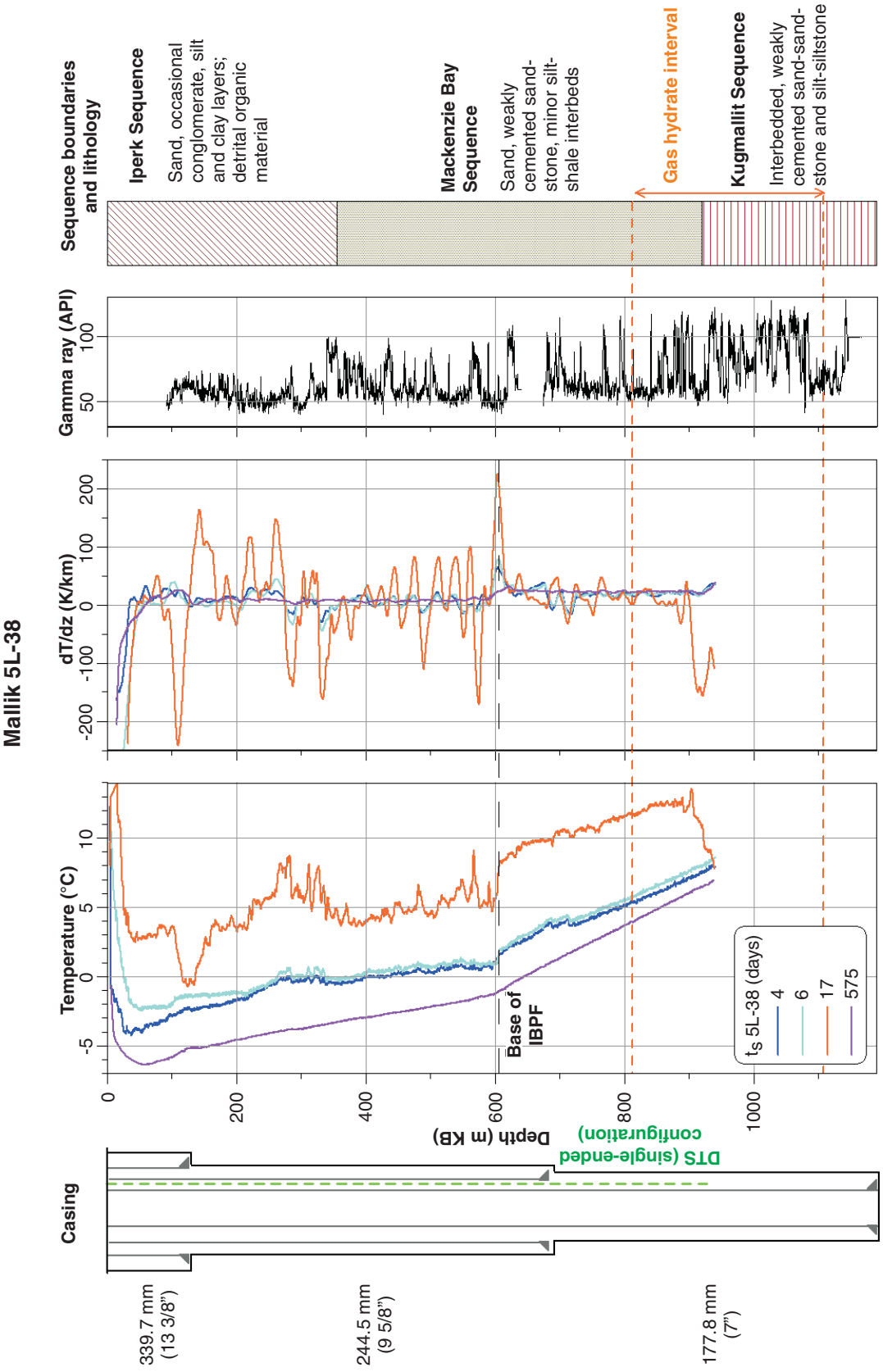

Figure 3. *Temperature profiles (T) and 20 m average temperature gradient (dT/dz) of the Mallik 5L-38 production well for successive times after completion of the well (t_S). The 17 day temperature profile shows remaining influence from preceded testing operations. IBPF: ice-bearing permafrost. The gamma-ray log (GR) was run open-hole; permafrost interval may be affected by strong washouts. Sequence boundaries and lithological description* modified from *Dallimore et al. (1999). Depth in metres below kelly bushing (m KB).*

Table 1. Summary of DTS installation and logging schedule for Mallik 2002. Dates are in year.month.day format.

	3L-38	4L-38	5L-38	Total
Begin drilling	2001.12.25	2002.01.11	2002.01.25	
End drilling	2002.01.06	2002.01.21	2002.02.22	
End cementation	2002.01.07	2002.01.22	2002.02.23	
Start DTS logging	2002.01.10	2002.01.25	2002.02.24	
End DTS logging	2002.03.12	2002.03.12	2002.03.12	
1st post-field DTS survey	2002.10.06–07	2002.10.06–07	No data	
2nd post-field DTS survey	2003.09.19–21	2003.09.19–21	2003.09.19–21	
Number of profiles	9231	5150	4554	**18 935**
Max. depth DTS (m KB)	1157.84	1158.32	938.61	
Processing method	Double ended	Single ended	Single ended	
Data points (dz = 0.25 m)	10 514	7387	4386	
Measurements (total)	$7.5x10^7$	$3.8x10^7$	$2.0x10^7$	**$1.33x10^8$**

the DTS cables were secured and left accessible during the abandonment of the wells. The surface ends of the sensor cables were stored in custom-designed steel boxes on site.

Temperature logging schedule

After the completion of the wells, continuous monitoring of the well temperatures was performed over a period of up to 61 days from January to March 2002. The DTS logging was started one to two days after completion of the respective well. Temperature profiles were recorded with sampling intervals of 0.25 m and 5 minutes. Table 1 contains details of the DTS installation and the logging schedule, as well as the amount of recorded temperature data.

Two further DTS surveys were carried out during subsequent field trips to the Mallik site on October 6 and 7, 2002, and September 19–21, 2003. During the October 2002 field trip, temperature profiles from the two observation wells were obtained, but the Mallik 5L-38 well was not accessible due to flooding of the well site. During the September 2003 field trip, data from all three wells were collected.

RESULTS AND DISCUSSION

Excerpts from the recorded temperature data are displayed in Figures 1, 2, and 3 as temperature profiles for successive points in time after the cementing of the wells (shut-in time, t_s). Details concerning the processing of the DTS data are documented within the Appendix below. The temperature gradient at every data point was calculated from the slope of the temperature profiles over 5 m, 10 m, and 20 m intervals, as indicated in the respective figure captions. This smoothing of the temperature gradients reduced the influence of the scatter of the raw temperature data due to instrumental noise. The size of the averaging interval was further adjusted to the scale of the respective diagram for clarity. For the Mallik 3L-38 and 4L-38 observation wells, cased-hole gamma-ray logs are displayed, which were recorded by the cement bond tool (CBT). The gamma-ray logs for the Mallik 5L-38 well were recorded during the open-hole logging program of the permafrost and subpermafrost sections.

After the October 2002 field trip, it had been discovered that the original calibration had obviously changed due to a modification of the DTS instrument, and the collected temperature data was offset up to several degrees. Although this offset could be determined and corrected by subsequent measurements, the October 2002 temperature data is only shown with dashed lines in Figures 1–3. Prior to the September 2003 field trip, a new calibration of the DTS instrument was performed and the calibration was verified by on-site measurements under controlled conditions.

Natural geothermal field and thermal rock properties

As a result of the thermal disturbance due to the drilling process, a continuous process of equilibration of the borehole temperature to the temperature of the surrounding formation can be observed during the 21 month logging period between January 2002 and September 2003 (Fig. 1, 2, 3). As will be shown below in the 'Drilling-induced temperature changes' section, the September 2003 temperature profiles have returned close to equilibrium with the formation temperature and the measured changes of temperature with depth are approximately equal to the geothermal gradient.

According to Fourier's equation, the rate of conductive heat flow per unit area $\dot{Q}$ (W/m^2) is equal to the product of thermal conductivity λ (W/m•K) and the change of temperature dT (K) over the distance dz (m):

$$\dot{Q} = -\lambda \frac{dT}{dz} \qquad (1)$$

Therefore, assuming constant heat flow by conduction, the temperature gradient is inversely proportional to thermal conductivity, and local changes of the geothermal gradient are correlated with changes of the bulk-rock thermal conductivity of the formation. In order to derive implications on the bulk-rock thermal conductivity of the formation, only the September 2003 'near equilibrium' temperature profiles are considered in the following discussion.

The September 2003 temperature profiles of the three wells all show very similar characteristics. Near the surface to a depth of about 80 m the temperature profiles exhibit curvature

attributable to the annual and recent (several decades) changes of surface temperature (e.g. Lachenbruch and Marshall, 1986). The temperature field in the deeper subsurface is characterized by a pronounced increase of the geothermal gradient at the base of the ice-bearing permafrost below about 600 m depth (Fig. 1, 2, 3). The mean temperature gradient within the Mackenzie Bay Sequence rises from 7.4–7.9 K/km above the permafrost base to 23.5–24.1 K/km in the ice-free sediment layers below (Fig. 4; Table 2). Since there is no apparent change in lithology at this depth (Fig. 4), the sharp increase in gradient can be attributed to a change of the bulk-rock thermal conductivity resulting from the contrast of the thermal conductivity of the pore fluid in frozen (ice: 2.2 W/m•K) and unfrozen (water: 0.6 W/m•K) state.

Below about 920 m, the geothermal gradient shows distinct variations and locally increases over 40 K/km. The onset of this interval with zones of increased geothermal gradient appears in all three wells and correlates with the boundary between the Mackenzie Bay and Kugmallit sequences, which at the Mallik L-38 well appears at a depth of 918 m below ground level (Dallimore and Collett, 1999). Individual peaks of the geothermal gradient are again showing good correlation between the Mallik 3L-38 and 4L-38 wells, and local differences can be attributed to lateral changes in lithology which can be derived by comparison of the gamma-ray logs.

Figure 5 shows a detail of the 10 m average temperature gradients and the gamma-ray log of the Mallik 3L-38 well, as well as an estimate of the gas hydrate saturation, based on the difference

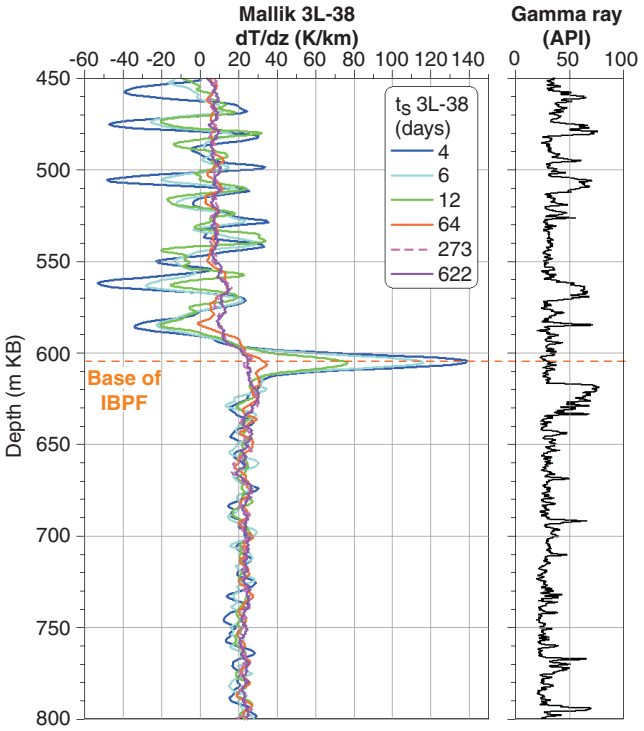

Figure 4. *Detail of 10 m average temperature gradients (dT/dz) and gamma-ray log, Mallik 3L-38 observation well, at the base of the ice-bearing permafrost (IBPF). Depth in metres below kelly bushing (m KB).*

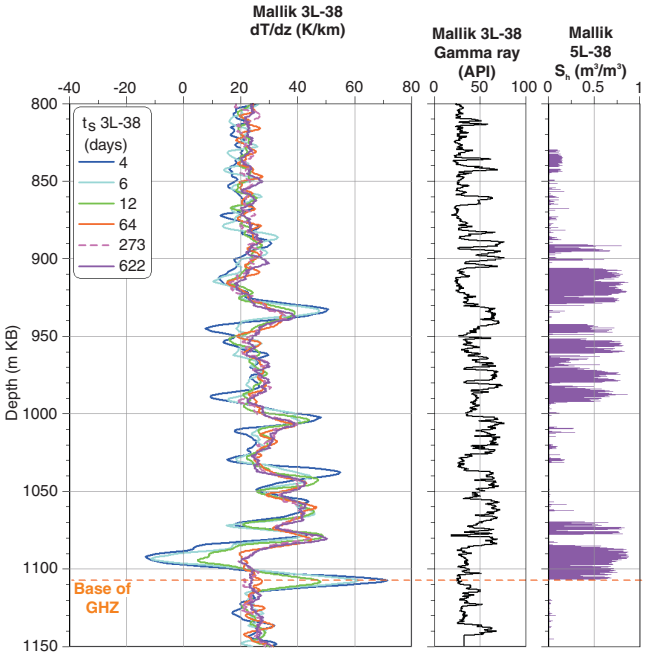

Figure 5. *Detail of 10 m average temperature gradients (dT/dz) and gamma-ray log, Mallik 3L-38 observation well, within the zone of the gas hydrate occurrences (GHZ). Gas hydrate saturation (S_h, fraction of total porosity) estimated from difference of density- and NMR-porosity logs from the 5L-38 well (see Kleinberg et al., 2005). Depth in metres below kelly bushing (m KB).*

Table 2. Temperature profile data and depth (in metres below kelly bushing: m KB) of permafrost and gas hydrate occurrences; IBPF = ice-bearing permafrost; GHZ = zone of the gas hydrate occurrences. No temperature data could be collected from base of gas hydrate zone in Mallik 5L-38.

	3L-38	4L-38	5L-38
Mean temperature gradient, 360–580 m KB, Sept. 2003 (K/km)	7.9	7.4	7.8
Mean temperature gradient, 620–900 m KB, Sept. 2003 (K/km)	23.5	24.1	23.6
Base of IBPF (m KB)	604 ± 3.5	609 ± 3.5	605 ± 3.5
Base of GHZ (m KB)	1108 ± 3.5	1109 ± 3.5	-

of the density- and NMR-porosity logs of the Mallik 5L-38 well (Kleinberg et al., 2005). As commonly observed, the geothermal gradient correlates with the gamma-ray log. Sand-dominated units, marked by low gamma-ray intensities, characteristically have a higher thermal conductivity than silt- or clay-dominated units with high gamma-ray intensities. In contrast to this, there is no apparent correlation of the temperature gradient and the estimated gas hydrate saturation. In order to examine the interrelation of the temperature gradient (dT/dz), the gamma-ray intensity (GR), and the gas hydrate saturation (S_h) in further detail, crossplots of 0.25 m interval data between 830 m and 1142 m are presented in Figure 6. Because no temperature data of the Mallik 5L-38 well could be collected below a depth of about 939 m, the average of the temperature gradients from the Mallik 3L-38 and 4L-38 wells was used for this analysis.

Figure 6a shows a crossplot of dT/dz and GR, with S_h indicated by the colour code (blue: low S_h, red: high S_h). Although there is no direct physical relationship between dT/dz and GR, the positive correlation between these quantities can be explained by the linkage through thermal conductivity described above. Variations in S_h do not result in an obvious systematic deviation from this correlation. There is, however, an accumulation of data points with high S_h values within the low temperature gradient and low gamma-ray intensity region. This indicates that the gas hydrate has preferentially accumulated within the sand-dominated units, which is also obvious from the crossplot of GR and S_h (Fig. 6c), which displays that high S_h values mostly occur together with low GR values. Figure 6b again displays no clear correlation between dT/dz and S_h. The presented evidence implies that at the Mallik site even high gas hydrate saturations of up to 90% of the pore space only have a minor effect on the bulk-rock thermal conductivity as compared to the effect of changes in lithology. In order to quantify changes of the thermal conductivity as a result of the presence of gas hydrate in the order of 30%, as observed by Stoll and Bryan (1979), direct measurements of thermal conductivity on field samples under in situ conditions would be required.

Drilling-induced temperature changes

The variation of temperature over time exhibits patterns of superimposed cooling and warming processes, which are related to different phases of the drilling of the well. The drilling operations lasted over a total period of 13 days for the Mallik 3L-38 well, and 11 days for the Mallik 4L-38 well from spud-in to cementing of the wells (Table 1). In the Mallik 5L-38 well, which was drilled with a larger diameter and cored in the interval between 886 m and 1151 m, drilling operations lasted a total of 29 days, which is more than twice as long as in the two observation wells.

The drilling of the permafrost and gas hydrate layers required that the borehole was not excessively heated during the drilling procedure, and the drilling mud was cooled to temperatures between –2°C and 4°C (Takahashi et al., 2005). As a consequence of the temperature difference between the formation and the drilling mud, the formation was warmed in the upper section and cooled in the lower section of the borehole during the drilling period. This pattern of thermal disturbance is typically observed in rotary-drilled wells (Bullard, 1947). After the drilling, the cementing of the casing caused an increase of temperature along the entire depth of the wells due to the release of the heat of hydration.

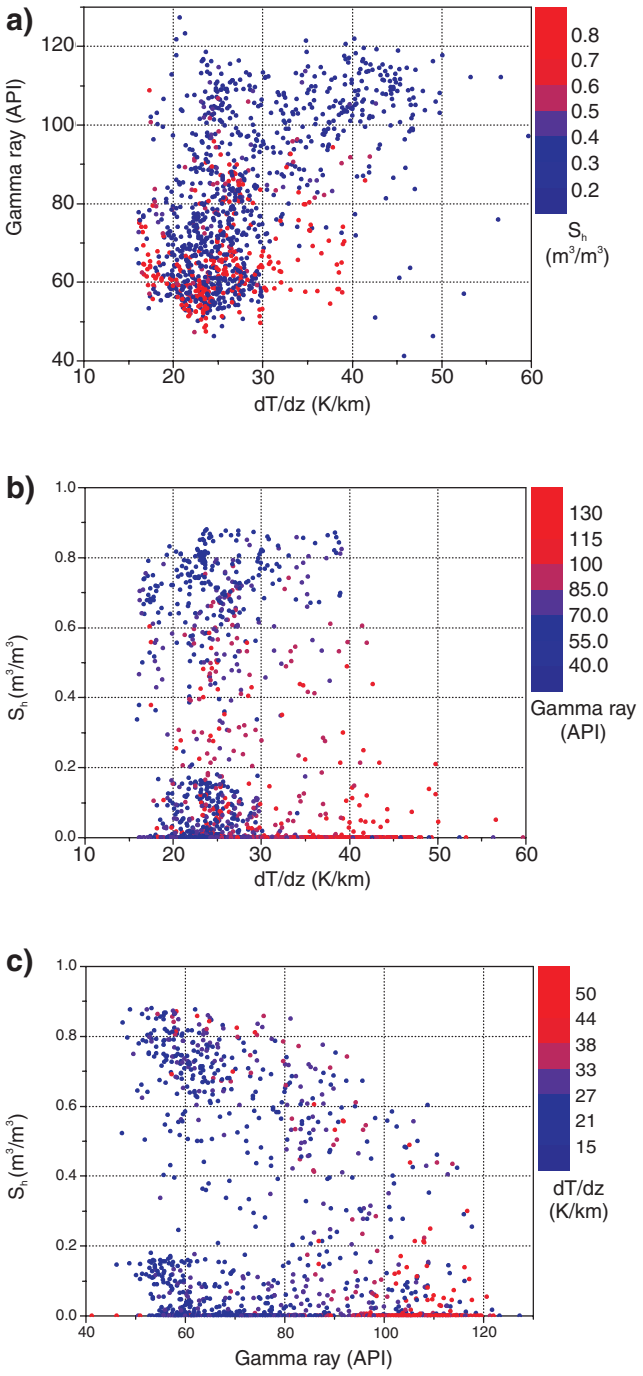

Figure 6. a), b), c) *Crossplots of the 5 m average mean temperature gradient of the 3L-38 and 4L-38 wells (dT/dz), gamma-ray intensity (GR), Mallik 5L-38 well, and gas hydrate saturation (S_h), estimated from Mallik 5L-38 well logs (see Fig. 5 and text for further details). Depth interval: 830–1142 m below kelly bushing.*

Despite the complex processes, it has been shown that under certain conditions the process of heat transfer during drilling can be approximated by an idealized line-source model (e.g. Bullard, 1947; Lachenbruch and Brewer, 1959). For shut-in times after the end of drilling, t_s, which are large relative to the time of circulation, t_c, the temperature along the borehole can be approximated by

$$T(t_s) = A \bullet \ln\left(1 + \frac{t_c}{t_s}\right) + T_\infty \quad (2)$$

where T_∞ is the undisturbed formation temperature and A is a constant, which in the ideal case would be given by

$$A = \frac{Q}{4\pi\lambda} \quad (3)$$

where Q is the rate of heat exchange during drilling per unit length of the borehole, and λ is the thermal conductivity of the surrounding formation.

The minimum time required for the validity of equation 2 is determined from the departure of the real drilling process from the constant-source model. After this time, a plot of the observed temperature after shut-in of the well $T(t_s)$ against $\ln(1+t_c/t_s)$ should yield a straight line of slope A and a value of T_∞ at $\ln(1+t_c/t_s) = 0$ (i.e. $t_s \rightarrow \infty$). The mobilization of latent heat in the permafrost and gas hydrate intervals during and after drilling is further limiting the applicability of this method, but it has been shown (Lachenbruch et al., 1982) that even for cases involving substantial degradation of permafrost during drilling, the straight-line slope is again recovered after sufficient time.

'Horner plots' of the type described above for various depths are presented in Figure 7 and 8. For this analysis it was assumed that the heat source at a particular depth had lasted from the time when the drill bit had first reached this depth until the end of the cementing of the wells (Table 1). The resulting circulation times, t_c for the chosen depth are ranging from about 12 days in the upper part of the borehole to about 2 days in the lower part (Tables 3, 4). Because of this variation of the circulation times, simultaneous measurements at different depths plot at different positions on the abscissa on Figures 7 and 8.

The observed temperature changes after the cementing of the wells depict the sequence of events and the amount of heat exchanged between the borehole and the surrounding formation during drilling. In the initial period, the temperature along the entire well decreases as a result of the dissipation of the heat of hydration released during the setting of the cement. In the following time, the temperature recovery in the upper and lower part of the borehole shows different trends: at depths greater than about 800 m, the part of the borehole which was subject to cooling during the drilling of the well, temperature is again increasing. In contrast to this, the interval above about 700 m was warmed during drilling, and the cooling after the initial period continues. The linear fits were applied to the data after minimum shut-in times $t_{s,min}$ ranging

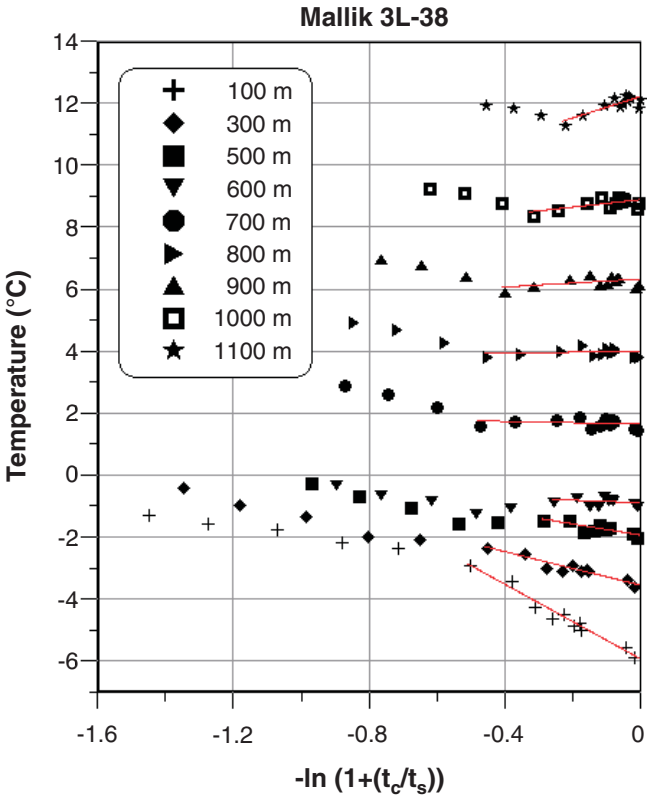

Figure 7. *'Horner plot' of temperature variation over time for various depths, Mallik 3L-38 observation well. Linear fits displayed with red lines. t_c: circulation time, t_s: shut-in time.*

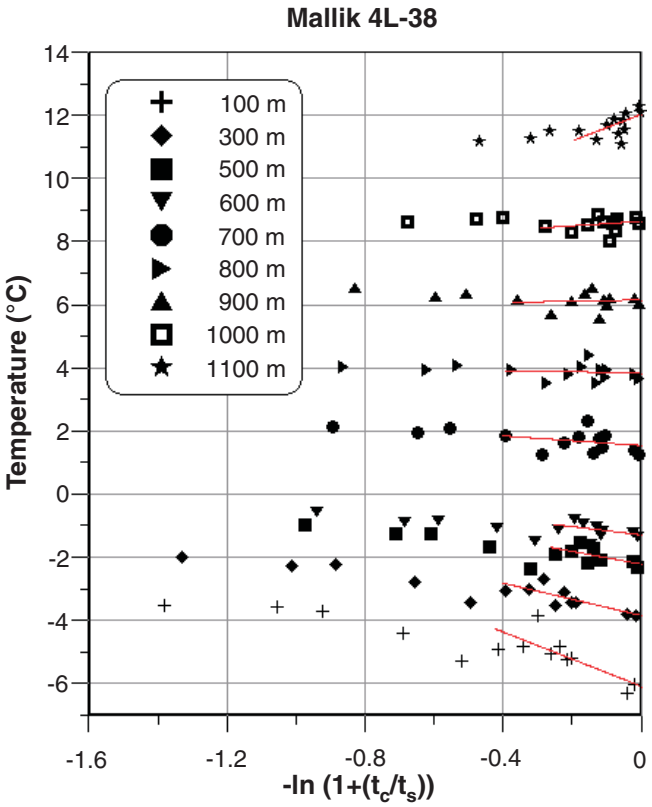

Figure 8. *'Horner plot' of temperature variation over time for various depths, Mallik 4L-38 observation well. Linear fits displayed with red lines. t_c: circulation time, t_s: shut-in time.*

from about 9 days to about 21 days. Tables 3 and 4 additionally list the corresponding dimensionless time t_s/t_c and the corresponding value on the abscissa (Fig. 7, 8) of the 'Horner plots', $t_{h, min}$. Because of the lingering influence due to the refreezing of permafrost, data from the permafrost interval generally could only be matched to a straight-line fit after shut-in times that were longer than for the interval below. The parameters A and T_∞ resulting from the linear fits, as well as the temperatures measured during the September 2003 survey $T_{Sept. 03}$, and the deviation from T_∞, dT, are presented in Tables 3 and 4.

The different slopes of the temperature curves with time within the 'Horner plots' clearly show the influence of variations of the heat source during the drilling process and effects that can be related to the mobilization of latent heat. While for the Mallik 3L-38 well a rather systematic deviation from the ideal case can be observed, the temperatures from the Mallik 4L-38 and 5L-38 wells show further influences: the removal of a spurious cement plug at about 850 m depth required a further two-day drilling operation at the Mallik 4L-38 well, lasting from day 26 to day 28. During this time, drilling mud was circulated with temperatures between 13°C and 20°C. The elevated temperatures resulting from this additional drilling operation are mostly evident in the upper 100 m of the well (Fig. 2, 49-day temperature profile; Fig. 5). As a consequence of the longer drilling time and the larger drill-bit diameter, the thermal disturbance of the Mallik 5L-38 well was much stronger than in the observation wells (Fig. 3). Further perturbations of the Mallik 5L-38 well temperatures were caused due to the extensive logging, coring, and testing program. Therefore the temperature data of the Mallik 5L-38 well was not evaluated within this analysis.

The analysis of the temperature data from the Mallik 3L-38 and 4L-48 wells using the 'Horner plot' method shows that the well temperatures measured during the September 2003 survey have returned to close to equilibrium with the formation temperatures. The deviation from thermal equilibrium is ± 0.1°C (Tables 3, 4) and within measurement accuracy. For wells or sections of wells where no mobilization of latent heat due to phase changes occurs, Bullard (1947)

Table 3. 'Horner plot' data, Mallik 3L-38; t_c, circulation time; $t_{s, min}$, minimum shut-in time for 'Horner plot' evaluation; t_s/t_c, ratio of shut-in time:circulation time; $t_{h, min}$, minimum 'Horner time' ($t_h = \ln(1 + t_c/t_s)$); A, slope of linear fit in 'Horner plot'; T_∞, undisturbed formation temperature, estimated from 'Horner plot'; $T_{Sept. 03}$, temperature measured during September 2003 survey; dT, deviation of temperature measured in September 2003 from estimated equilibrium temperature ($T_\infty - T_{Sept. 03}$)

Depth (m KB)	t_c (d)	$t_{s, min}$ (d)	t_s/t_c	$t_{h, min}$	A	T_∞(°C)	$T_{Sept.03}$ (°C)	dT (°C)
100.13	12.37	18.86	1.53	0.50	6.02	-5.97	-5.88	-0.09
200.12	11.87	18.86	1.59	0.49	2.87	-4.41	-4.50	0.09
300.11	10.81	18.86	1.74	0.45	2.72	-3.59	-3.64	0.05
400.10	6.47	18.86	2.91	0.30	2.69	-2.74	-2.81	0.07
500.09	6.21	18.86	3.04	0.28	1.81	-1.97	-2.06	0.09
600.08	5.52	18.86	3.42	0.26	0.40	-0.92	-1.04	0.12
700.07	5.29	8.79	1.66	0.47	0.21	1.62	1.43	0.19
800.06	5.03	8.79	1.75	0.45	-0.14	3.96	3.82	0.14
900.05	4.36	8.79	2.02	0.40	-0.64	6.29	6.10	0.19
1000.04	3.27	8.79	2.69	0.32	-1.20	8.85	8.74	0.11
1100.03	2.19	8.79	4.01	0.22	-3.46	12.19	12.09	0.10

Table 4. 'Horner plot' data, Mallik 4L-38; t_c, circulation time; $t_{s, min}$, minimum shut-in time for 'Horner plot' evaluation; t_s/t_c, ratio of shut-in time:circulation time; $t_{h, min}$, minimum 'Horner time' ($t_h = \ln(1 + t_c/t_s)$); A, slope of linear fit in 'Horner plot'; T_∞, undisturbed formation temperature, estimated from 'Horner plot'; $T_{Sept. 03}$, temperature measured during September 2003 survey; dT, deviation of temperature measured in September 2003 from estimated equilibrium temperature ($T_\infty - T_{Sept. 03}$).

Depth (m KB)	t_c (d)	$t_{s, min}$ (d)	t_s/t_c	$t_{h, min}$	A	T_∞(°C)	$T_{Sept.03}$ (°C)	dT (°C)
100.05	10.84	21.14	1.95	0.41	4.31	-6.11	-6.02	-0.09
200.09	10.45	21.14	2.02	0.40	3.71	-4.71	-4.66	-0.05
300.13	10.14	21.14	2.08	0.39	2.57	-3.87	-3.85	-0.02
400.18	6.17	21.14	3.43	0.26	3.81	-3.02	-3.04	0.02
500.22	6.00	21.14	3.53	0.25	2.02	-2.25	-2.31	0.06
600.01	5.69	21.14	3.72	0.24	1.33	-1.32	-1.34	0.02
700.05	5.28	10.91	2.07	0.39	0.76	1.51	1.24	0.27
800.09	5.00	10.91	2.18	0.38	0.18	3.81	3.65	0.16
900.13	4.71	10.91	2.32	0.36	-0.20	6.12	6.01	0.11
1000.17	3.52	10.91	3.10	0.28	-0.71	8.61	8.59	0.01
1100.21	2.19	10.91	4.99	0.18	-4.19	11.98	12.10	-0.12

showed that about 10 to 20 times the time taken to drill at a particular depth is required for the disturbance to decrease to 1% of its initial value. Based on the recorded mud temperatures at Mallik, the maximum of the initial temperature disturbance can be estimated as about 15°C. Temperatures measured in October 2002 follow the completion of drilling operations by a period of time equal to about 21 times the duration of drilling. Then according to Bullard's (1947) result, well temperatures should be within 0.15°C of thermal equilibrium, which is in agreement with the results for the 'Horner plot' analysis. Within measurement accuracy, the temperatures of the September 2003 measurement have reached thermal equilibrium, except for the upper part of the permafrost section of the Mallik 5L-38 well, where a remaining disturbance of the temperature profile around 130 m is obvious (Fig. 3). Further temperature changes after the September 2003 measurement can be expected here.

Transient heat flow and phase changes

The disturbed temperature profiles exhibit specific patterns, which are related to the mobilization of latent heat during the melting and refreezing of permafrost (e.g. Lachenbruch and Brewer, 1959; Lachenbruch et al., 1982) and the decomposition of gas hydrate as a result of the drilling and completion of the wells. In this study, these patterns were used as indicators of the location of the base of the ice-bearing permafrost and gas hydrate occurrences.

Especially during early times after the end of drilling, the disturbed temperature profiles are characterized by almost isothermal sections within the permafrost interval, followed by a gradual increase in temperature in the deeper subsurface below (Fig. 1, 2, 3). The transition between these zones is marked by a sharp rise in temperature over a depth interval of a few metres at about 600 m, which is gradually diminishing over time. During drilling, the rise of temperature within permafrost is impeded by the latent heat used to melt the frozen pore fluid, whereas the rise of temperature beneath permafrost is not limited in this way (Lachenbruch and Brewer, 1959; Lachenbruch et al., 1982). The resulting transient temperature step marks the base of the ice-bearing permafrost layer and is an effect typical of many wells drilled in permafrost (Taylor, 1979). A similar effect can be observed in the depth interval below 1100 m (Fig. 1, 2). By analogy to the permafrost feature, this indicates that decomposition of gas hydrate had occurred at the base of the gas-hydrate-bearing zone, probably as a result of a release of heat of hydration after cementing the wells.

Being close to thermodynamic equilibrium, the intervals immediately above the base of the ice-bearing permafrost and gas hydrate occurrences are mostly prone to melting or decomposition, respectively. Even small changes of the pressure and temperature conditions can result in phase changes. During the supply of heat, the consumption of latent heat at the phase change or decomposition temperature is leading to the development of isothermal sections of the temperature profiles in the permafrost and gas hydrate intervals, which are subject to phase changes. In contrast to this, the temperatures in the zones immediately below the melting permafrost or decomposing gas hydrate interval are increasing according to the thermal diffusivity of the rock. In comparison to the temperature profiles, the plots of the disturbed temperature gradients (Fig. 4, 5) accentuate this effect: within the zones subject to phase changes, the temperature gradients decrease and reach a local minimum, after which the gradients strongly increase with depth (temperature step), before they return to a value close to the geothermal gradient underneath the transition zones. The transition zones between the ice-bearing and non-ice-bearing strata (Fig. 4), and between the gas-hydrate-bearing and non-gas-hydrate-bearing strata (Fig. 5) are therefore marked by a sinusoidal signature in the temperature-depth gradient. This 'pseudo-discontinuity' of the temperature gradient and the related temperature step are both gradually decreasing over time as the thermal disturbance dissipates.

The temperature steps occurred within depth intervals of about 7 m. Within these transition zones, the locations of the local maxima of the temperature gradients were used to determine the position of the base of the ice-bearing permafrost and the gas hydrate occurrences (Table 2). With respect to the thickness of the transition zones, an uncertainty of ± 3.5 m should be assumed for the given depth values for the positions of the respective interfaces. Moreover, at least around the base of the ice-bearing permafrost, a gradual transition zone, of variable thickness, with coexisting ice and water within the pore space will probably exist.

The depth to the base of the ice-bearing permafrost increases from 604 ± 3.5 m at Mallik 3L-38 to 609 ± 3.5 m at Mallik 4L-38. These values generally agree with previous determinations of the depth to the base of the ice-bearing permafrost for the Mallik region (e.g. Judge, 1987), but they are about 30 m less than the depths determined for the approximately 100 m distant Mallik L-38 and 2L-38 wells, which were estimated from geophysical well logs (Dallimore and Collett, 1999; Dallimore et al., 1999), since precision well temperatures were not available.

The depth to the base of the gas hydrate occurrence increases from 1108 ± 3.5 m at the Mallik 3L-38 well to 1109 ± 3.5 m at the Mallik 4L-38 well, and shows the same trend as the depth to the ice-bearing permafrost. A similar determination of the base of the gas hydrate occurrence at the Mallik 5L-38 well was not possible because temperatures could only be measured to a depth of about 940 m, but the temperature-derived depths to the base of the gas hydrate occurrences for the Mallik 3L-38 and 4L-38 wells correlate well with the gas hydrate saturation estimated from the density- and NMR-porosity logs for the Mallik 5L-38 well at about 1107 m.

CONCLUSIONS

The permanent installation of fibre-optic distributed temperature-sensing cables behind the well casing proved to be successful for temperature monitoring in boreholes, even under the extreme conditions of an arctic environment. The measured temperature profiles enabled the determination of the formation temperature, and the derivation of new implications for

the distribution of permafrost and gas hydrate occurrences, as well as the thermal properties of gas-hydrate-bearing sediments at the Mallik site.

1) For the Mallik 2002 wells, the dissipation of the thermal disturbances caused by the drilling and completion of the wells still continued after a period of 64 days, which corresponds to five times the drilling period. After about 21 months, which corresponds to over 48 times the drilling period, the temperature of the Mallik 3L-38 and 4L-38 wells had returned close to undisturbed conditions, with an estimated deviation of ± 0.1°C from equilibrium. Within the upper approximately 200 m of the Mallik 5L-38 well some remaining influence of the thermal disturbance can be detected.

2) The temperature profiles exhibit features typical of wells drilled in permafrost, such as a pronounced step-like increase of temperatures at the base of the ice-bearing permafrost, within short times after the completion of the wells. The depths to the base of the ice-bearing permafrost derived from this characteristic feature increase from 604 ± 3.5 m in the Mallik 3L-38 well to 609 ± 3.5 m in the Mallik 4L-38 well.

3) For the first time, a similar effect as described under number 2) above, caused by the consumption of latent heat by the decomposition of gas hydrate during completion of the wells, was detected at the base of the gas hydrate occurrences. This temperature log-derived depth of the base of the gas hydrate occurrences corresponds well to the depth estimated from other geophysical well logs and ranges between 1108 ± 3.5 m and 1109 ± 3.5 m for the Mallik 3L-38 and 4L-38 wells, respectively.

4) Changes of the geothermal gradient are linked to variations in lithology and the ice content of the sediments. The influence of the gas hydrate content on the bulk-rock thermal conductivity, nevertheless, only plays a minor role when compared to lithological changes of the rock matrix.

ACKNOWLEDGMENTS

This is publication no. GEOTECH-58 of the programme GEOTECHNOLOGIEN of BMBF and DFG, grant G0556A. The Mallik 2002 Gas Hydrate Production Research Well Program participants include seven partners: Geological Survey of Canada (GSC), Japan National Oil Corporation (JNOC), GeoForschungsZentrum Potsdam (GFZ), United States Geological Survey (USGS), United States Department of Energy (USDOE), India Ministry of Petroleum and Natural Gas (MOPNG), BP–ChevronTexaco–Burlington joint venture parties and was supported by the International Continental Scientific Drilling Program (ICDP). The excellent co-operation with the drilling operations team and the AKITA 15 drilling crew during the field experiment is greatly acknowledged. The Geological Survey of Canada and the Inuvik Research Centre have provided invaluable logistical support for the October 2002 and September 2003 post-field-site visits. The authors would like to thank the technical staff at GFZ Potsdam, C. Karger, S. Meyhöfer, and T. Schläfke, for their support during the DTS calibration measurements. A.E. Taylor and an anonymous reviewer contributed valuable comments and suggestions for the preparation of the final manuscript.

REFERENCES

Bullard, E.C.
1947: The time necessary for a borehole to attain temperature equilibrium; Monthly Notices of the Royal Astronomical Society, Geophysical Supplement, v. 5, no. 5, p. 127–130.

Dallimore, S.R. and Collett, T.S.
1999: Regional gas hydrate occurrences, permafrost conditions, and Cenozoic geology, Mackenzie Delta area; *in* Scientific Results from JAPEX/ JNOC/GSC Mallik 2L-38 Gas Hydrate Research Well, Mackenzie Delta, Northwest Territories, Canada, (ed.) S.R. Dallimore, T. Uchida, and T.S. Collett; Geological Survey of Canada, Bulletin 544, p. 31–43.

Dallimore, S.R. and Collett, T.S.
2005: Summary and implications of the Mallik 2002 Gas Hydrate Production Research Well Program; *in* Scientific Results from the Mallik 2002 Gas Hydrate Production Research Well Program, Mackenzie Delta, Northwest Territories, Canada, (ed.) S.R. Dallimore and T.S. Collett; Geological Survey of Canada, Bulletin 585.

Dallimore, S.R., Collett, T.S., and Uchida, T.
1999: Overview of science program, JAPEX/JNOC/GSC Mallik 2L-38 gas hydrate research well; *in* Scientific Results from JAPEX/JNOC/GSC Mallik 2L-38 Gas Hydrate Research Well, Mackenzie Delta, Northwest Territories, Canada, (ed.) S.R. Dallimore, T. Uchida, and T.S. Collett; Geological Survey of Canada, Bulletin 544, p. 11–17.

Förster, A., Schrötter, J., Merriam, D.F., and Blackwell, D.D.
1997: Application of optical-fiber temperature logging – an example in a sedimentary environment; Geophysics, v. 62, no. 4, p. 1107–1113.

Hancock, S., Collett, T.S., Dallimore, S.R., Satoh, T., Inoue, T., Huenges, E., Henninges, J., and Weatherill, B.
2005: Overview of thermal-stimulation production-test results for the JAPEX/JNOC/GSC et al. Mallik 5L-38 gas hydrate production research well; *in* Scientific Results from the Mallik 2002 Gas Hydrate Production Research Well Program, Mackenzie Delta, Northwest Territories, Canada, (ed.) S.R. Dallimore and T.S. Collett; Geological Survey of Canada, Bulletin 585.

Hartog, A. and Gamble, G.
1991: Photonic distributed sensing; Physics World, v. 3, p. 45–49.

Hurtig, E., Schrötter, J., Grosswig, S., Kühn, K., Harjes, B., Wieferig, W., and Orrell, R.P.
1993: Borehole temperature measurements using distributed fibre optic sensing; Scientific Drilling, v. 3, no. 6, p. 283–286.

Judge, A.S., Pelletier, B.R., and Norquay, I.
1987: Permafrost base and distribution of gas hydrates; *in* Marine Science Atlas of the Beaufort Sea — Geology and Geophysics, (ed.) B.R. Pelletier; Geological Survey of Canada, Miscellaneous Report 40, p. 39.

Kleinberg, R.L., Flaum, C., and Collett, T.S.
2005: Magnetic resonance log of JAPEX/JNOC/GSC et al. Mallik 5L-38 gas hydrate production research well: gas hydrate saturation, growth habit, and relative permeability; *in* Scientific Results from the Mallik 2002 Gas Hydrate Production Research Well Program, Mackenzie Delta, Northwest Territories, Canada, (ed.) S.R. Dallimore and T.S. Collett; Geological Survey of Canada, Bulletin 585.

Lachenbruch, A.H. and Brewer, M.C.
1959: Dissipation of the temperature effect of drilling a well in Arctic Alaska; United States Geological Survey, Bulletin 1083-C, p. 73–109.

Lachenbruch, A.H and Marshall, B.V.
1986: Changing climate: geothermal evidence from permafrost in the Alaskan Arctic; Science, v. 234, p. 689–696.

Lachenbruch, A.H., Sass, J.H., Marshall, B.V., and Moses, T.H., Jr.
1982: Permafrost, heat flow, and the geothermal regime at Prudhoe Bay, Alaska; Journal of Geophysical Research, v. 87, p. 9301–9316.

Majorowicz, J.A. and Smith, S.L.
1999: Review of the ground temperatures in the Mallik field area: a constraint to the methane hydrate stability; *in* Scientific Results from JAPEX/JNOC/GSC Mallik 2L-38 Gas Hydrate Research Well, Mackenzie Delta, Northwest Territories, Canada, (ed.) S.R. Dallimore, T. Uchida, and T.S. Collett; Geological Survey of Canada, Bulletin 544, p. 45–56.

Majorowicz, J.A., Jones, F.W., and Judge, A.S.
1990: Deep subpermafrost thermal regime in the Mackenzie Delta basin, northern Canada – analysis from petroleum bottom-hole temperature data; Geophysics, v. 55, no. 3, p. 362–371.

Ruppel, C.
2000: Thermal state of the gas hydrate reservoir; *in* Natural Gas Hydrate in Oceanic and Permafrost Environments, (ed.) E.D. Max; Kluwer Academic Publishers, Dordrecht, The Netherlands, p. 29–42.

Stoll, D.R. and Bryan, G.M.
1979: Physical properties of sediments containing gas hydrates; Journal of Geophysical Research, v. 84, no. 4, p. 1629–1634.

Takahashi, H., Fercho, E., and Dallimore, S.R.
2005: Drilling and operations overview of the Mallik 2002 Production Research Well Program; *in* Scientific Results from the Mallik 2002 Gas Hydrate Production Research Well Program, Mackenzie Delta, Northwest Territories, Canada, (ed.) S.R. Dallimore and T.S. Collett; Geological Survey of Canada, Bulletin 585.

Taylor, A.E.
1979: Thermal regime modelled for drilling and producing in permafrost; Journal of Canadian Petroleum Technology, v. 18, no. 2, p. 59–66.

Taylor, A.E. and Judge, A.S.
1981: Measurement and prediction of permafrost thickness, arctic Canada; *in* Technical Papers, 51st Annual Meeting, Society of Exploration Geophysicists, v. 6, p. 3964–3977.

Waite, W.F., deMartin, B.J., Kirby, S.H., Pinkston, J., and Ruppel, C.D.
2002: Thermal conductivity measurements in porous mixtures of methane hydrate and quartz sand; Geophysical Research Letters, v. 29, no. 24, p. 82-1 to 82-4.

Wisian, K.W., Blackwell, D.D., Bellani, S., Henfling, J.A., Normann, R.A., Lysne, P.C., Förster, A., and Schrötter, J.
1998: Field comparison of conventional and new technology temperature logging systems; Geothermics, v. 27, no. 2, p. 131–141.

APPENDIX

Technical specifications, advantages, and problems of the DTS experiment design

The permanent installation of the DTS sensor cables outside the borehole casing has several advantages: the sensor cable is positioned close to the borehole wall, and temperature perturbations due to fluid-air convection or movement of logging tools inside the borehole are minimized. Full access to the borehole for other operations during temperature measurement is available and long-term observations in abandoned and sealed wells are possible.

The cable clamps, which were designed in collaboration with the drilling operations team (Takahashi et al., 2005), enabled the positioning of the cable around the perimeter of the casing and the protection against mechanical damage during the installation procedure. In the two observation wells, the DTS cables were installed down to a depth of about 1158 m. The production test well (Mallik 5L-38) was perforated within the interval between 907 m and 920 m with zero phase. In order to ensure a functioning sensor cable within the thermal stimulation zone, two separate cable lines at 180° spacing were installed down to a depth of about 987 m in the Mallik 5L-38 well. In the event that one of these cable lines would have been destroyed during perforation, temperature data still could have been collected from the second undamaged line. Because further perforations were performed at different levels below this depth, the sensor cables were not installed to greater depths.

The deployed DTS system can be operated in two different configurations, which are referred to as single-ended and double-ended processing modes. The double-ended mode yields higher quality temperature data with a reduction of the signal noise, and requires that both ends of the sensor cable are connected to the DTS instrument. In order to operate the DTS instrument in double-ended mode, the sensor cables in all wells were installed in a closed-loop configuration with a turn-around at the bottom.

The sensor cable, a graded index 50/125 fibre contained in a high-grade steel tubule with a kevlar and HDPE plastic jacketing (manufactured by Felten & Guilleaume Kabelwerke GmbH, Germany), was chosen according to the temperature range and the mechanical stress expected during deployment. During the Mallik field experiment the sensor cables were exposed to arctic surface temperatures as low as -45°C and downhole temperatures up to +60°C during the thermal stimulation test. After the installation, breaks of the optical fibres were detected at about 650 m in the Mallik 4L-38 well, and at about 762 m, 831 m, and 939 m in the Mallik 5L-38 well, which are attributed to mechanical stress downhole during the installation procedure. Despite the damages, temperatures in the Mallik 4L-38 well could still be measured down to the bottom of the well because the sensor cables were installed in the loop configuration described above and only one cable branch was broken. Measurements could still be performed in single-ended mode and the damage therefore only resulted in a partial reduction of data quality. In the Mallik 5L-38 well, temperatures could be measured in single-ended mode down to a maximum depth of about 939 m.

While the damage of the sensor cable in the Mallik 4L-38 well cannot be related to any specific feature of the well completion or lithology at this depth, or to irregularities during the installation procedure, the damages of the sensor cables in the Mallik 5L-38 well could have been caused by a steel object which was accidentally dropped into the borehole. Damages to the optical fibre have resulted in only a partial reduction of data quality, and the need for care during the installation procedure must be emphasized. In order to further reduce the risk of damage, a more robust cable make-up should be developed for installations of this particular type.

Processing of distributed temperature data

The temperature profiles were measured at variable intervals ranging from about one to five minutes, depending on the configuration. The temperature profiles displayed in this report were generated by averaging the measured temperatures over about two hour data acquisition intervals in order to achieve the best possible accuracy.

Depth values are correlated to the positions of the uppermost connector at the wellhead and the lowest connector to which the DTS cable is attached. A comparison of the length of the sensor cable and casing string shows that the length of the installed sensor cable exceeds the length of the casing string by about 7 m to 8 m, a result of the addition of small excess cable lengths between the cable clamps, which were used to attach the cable to the borehole casing within intervals of about 12 m. It is assumed that this over-length of the sensor cable, which represents 0.8% of the length of the casing string, is evenly distributed along the depth of the borehole; the measured depth values were corrected accordingly.

In the Mallik 5L-38 well, the exact position of the end of the sensor cable relative to the casing string was initially not known because both lines of the cable loop were interrupted. Here the depth values were correlated to the position of the perforated interval of the thermal stimulation zone, which could be detected clearly by the thermal signal of the perforation gun after the perforation was shot (*see also* Hancock et al., 2005).